Sixth International Symposium on Marine Propulsors
smp'19, Rome, Italy, May 2019

A Method for Rudder Force Calculation in the Design Process Considering Rudder-Propeller-Interaction

Björn Carstensen[1]

[1]Institute of Ship Design and Ship Safety, Hamburg University of Technology, Hamburg, Germany

ABSTRACT

This paper presents a method to quickly calculate the rudder forces including the interaction between rudder and propeller. The presented method couples and enhances two existing methods for the calculation of propeller and rudder forces. Since the method should be applied in the early design stage, the used methods need to be quick and therefore they both base on the potential theory. Firstly, the interaction between the different lifting surfaces is calculated iteratively with a lifting line approach, where each device is described by a lifting line. Afterwards, these results are used as initial values in a three dimensional panel method. After calculating the setup in the panel method, the results are used to improve the calculation of the lifting line. At the end, the pressure distribution on the rudder and the forces of the rudder are calculated using the panel method, whereas the forces and moments of the propeller are calculated with the lifting line. The paper presents results of the rudder-propeller interaction for the ahead condition in an exemplary case.

Keywords

Lifting line, panel method, rudder-propeller interaction, rudder design

1 INTRODUCTION

Due to strong competition in the maritime market and requirements from regulations regarding the energy efficiency, an efficient overall design of the propulsion devices is essential. Traditionally, each device is designed and produced by one manufacturer. The drawback thereof is that the interaction between the devices is not or just insufficiently considered. For a reliable prediction of the forces and a competitive design, the interaction between different lifting surfaces needs to be considered already during the early design. The main challenge during the early design stage is that many different and often changing configurations need to be calculated in a small amount of time. Therefore, the used methods need to produce quick and reliable results.

The configuration discussed in this paper is a rudder placed in the propeller slipstream without any further appendages, such as energy saving devices. By placing the rudder in the propeller slipstream, the maneuverability is enhanced, especially for slow speed maneuvering. Furthermore, the propulsive efficiency may increase for a good design through the bidirectional interaction between the rudder and the propeller. The propeller generates a non-uniform flow downstream at the rudder consisting of an axial and tangential part. Brunnstein (1968) analysed the interaction between the ship wake, propeller and rudder using lifting surface theory. In his work, the interaction of the rudder on the propeller is divided into two components. On the one hand, the rudder generates a transversal flow upstream at the propeller, which increases the propeller thrust. On the other hand, the finite thickness of the rudder leads to induced axial velocities contrary to the propeller induced axial velocity. Due to the reduction in magnitude of the axial flow upstream at the propeller, the angle of attack to the blade sections increases and consequently, the propeller thrust. The strength of the effects depends on the rudder geometry, the distance between propeller and rudder and the thrust loading of the propeller.

For the calculation of the mentioned configuration two different approaches exist. Either the interaction is covered by a simplified coupled model or the complete configuration is calculated in one setup. While the first approach is quicker, it often can just handle a one-way interaction. Examples for this approach in the rudder force calculation are constant body forces models in RANSE calculations or the modelling of the propeller as lifting line or surface when calculating the rudder with a panel method. For the second approach, the computational expense grows strongly due to its sheer size while it is still difficult to cover all interacting effects, which is why this approach is not suitable for the early design.

The discussed interaction and the configuration are part of several researches, where different approaches are used. An example of a coupled calculation is given by Brunnstein (1968), who developed a method based on lifting surface theory and analysed the interaction between the ship wake, propeller and rudder. As calculations were very expensive in his time, the work focuses on the theory but also presents one exemplary case. Another more recent example of a coupled calculation method is presented by Li (1996), who calculated the rudder with a vortex lattice method and the propeller with a bound vortex sheet. Another example of a coupled method on this topic is presented in (Berger et al 2015), where the propeller flow is calculated using a panel method and the rudder forces are calculated using a RANSE solver. The results were compared to full RANSE calculations. An overview covering the extensive experimental data of the propeller-rudder interaction carried out in the wind tunnel of Southampton is given by Molland & Turnock (2007).

This paper presents a method only using potential methods. Firstly, the interaction between the different lifting surfaces is calculated iteratively with a lifting line approach, where each device is described by a lifting line. The circulation of each device is determined and subsequently the induced velocities at the other lifting lines are calculated. This approach converges quickly and gives good results for the propeller forces and the flow field. Afterwards, these results are used in a three dimensional panel method for the rudder force calculation. The inflow from the propeller to the rudder in the panel method is taken from the results of the lifting line method. Moreover, the results of the lifting line method are used to calculate the shape of the rudder wake. At the end, the pressure distribution on the rudder and the forces of the rudder are calculated using the panel method, whereas the forces and moments of the propeller are calculated with the lifting line.

2 UNDERLYING CALCULATION METHODS

The presented method is part of the ship design environment E4, which, among others, is developed by the Institute of Ship Design and Ship Safety. The method couples and enhances existing validated methods for the calculation of propeller and rudder forces. All methods presented here base on potential flow theory, which assumes that the flow is incompressible, free of rotation and has no friction. In this chapter, only the most important aspects of the methods and important details for the coupling are presented. For a more extensive overview, please refer to the respective literature.

2.1 Lifting Line Method

The lifting line method, presented here, is based on (Isay 1964). The numerical implementation is described by Krüger & Abels (2017).

In the lifting line method, the lifting device is substituted by a bound vortex. As the circulation of the bound vortex changes along the bound vortex, free transversal vortex threads are induced due to Helmholtz's theorems. From Biot-Savart's law Isay (1964) derives the vortex-induced velocity field of the transversal vortices $\vec{U}_Q$ for a propeller:

$$\vec{U}_Q = \frac{1}{4\pi} \sum_{n=0}^{N-1} \int_{R_i}^{R_a} \int_0^{\infty} \frac{\partial \Gamma}{\partial s} \frac{\vec{r}_Q \times \mathrm{d}\vec{s}_Q}{|\vec{r}_Q|^3} \mathrm{d}s \qquad (1)$$

Where n is the index of the propeller blade under consideration and N the number of propeller blades. R_i and R_a designate the inner and outer radius of a propeller blade respectively. Γ denotes the circulation of a propeller blade section and s is the integration variable along a vortex thread. $\vec{r}_Q$ is the distance from the vortex thread to the point under consideration and $\mathrm{d}\vec{s}_Q$ is the infinitesimal length of a vortex thread.

Of special interest for later calculations are the induced velocities at the lifting line. For a stationary propeller, it is assumed that the induced velocities of the neighbouring blades cancel out at the blade under consideration. Goldstein (1929) solved equation (1) by adding a relation between a propeller of infinite blades and one with a finite number of blades:

$$u_Q\left(x=0,r\right) = \frac{r}{k_0} \frac{N\Gamma}{4\pi r} \frac{1}{\kappa} \qquad (2)$$

$$v_Q\left(x=0,r\right) = \frac{r}{k_0} \frac{N\Gamma}{4\pi r} \frac{1}{\kappa} \qquad (3)$$

Where u_Q is the induced axial velocity, v_Q the induced tangential velocity and k_0 is the pitch of the free vortex and κ is the Goldstein factor. The Goldstein factor describes the ratio between the peak of the velocity at a vortex and the mean velocity which is equivalent to the comparison of a propeller with infinite blade number and one with a finite amount of blades. The values for the Goldstein factor are tabulated for different numbers of blades and depending on the local radius r and the pitch of the free vortex k_0. To calculate the velocities at different x-positions, Lerbs (1955) suggested an improved procedure introducing tabulated induction factors for the axial velocity g_a and for the tangential velocity g_t:

$$u_Q\left(x,r\right) = u_Q\left(x=0,r\right)\left(1+g_a(x,r)\right) \qquad (4)$$

$$v_Q\left(x,r\right) = v_Q\left(x=0,r\right)\left(1+g_t(x,r)\right) \qquad (5)$$

For the analysis of multi-component propulsors, Krüger (2018) extended the Goldstein and induction factors for different positions in the slipstream, blade numbers from 1 to 8 and for non rotating lifting devices, such as rudders.

Furthermore, the suggested correction of Söding (1993) is applied for the induced velocities in the propeller slipstream. The correction depends on the axial position, the thrust loading, and the velocity. It corrects the diameter and the velocities of the slipstream due to continuity and turbulent mixing.

For the angle of the free vortices β_i holds:

$$\tan\left(\beta_i\right) = \frac{k_0}{r} = \frac{u_0 + u_Q}{\omega r + v_Q} \qquad (6)$$

with ω being the angular velocity of the propeller and u_0 being the axial inflow.

Following the airfoil theory of Prandtl & Betz (1927) and using equation (6), the circulation at a section is given by:

$$\Gamma(r) = \frac{\omega r \tan\delta_0 - u_0}{\frac{2}{c_a'}\frac{1}{c\cos\delta_0} + \frac{N}{4\pi r\kappa}\left(\tan\delta_0 + \frac{r}{k_0}\right)} \qquad (7)$$

With the angle of zero lift δ_0, the lift coefficient c_a' and the chord length c.

The problem in calculating the circulation in equation (7) is that the pitch of the free vortices depends on the induced velocities (see eq. (6)) which depend on the circulation (see eq. (2) and eq. (3)). This is why the circulation needs to be calculated in an iterative manner. In the beginning, the induced velocities in equation (6) are set to zero. Thereafter, the circulation is calculated and then the induced velocities are evaluated. Afterwards, the procedure starts again with the newly obtained induced velocities. This approach converges quickly and gives satisfying results for integral propeller values as thrust and torque. Moreover, the velocities in in the slipstream of the propeller and in front of the propeller can be calculated using this method.

The calculation of multi-component propulsors with a lifting line approach leads to a simultaneous boundary value problem at the propeller and rudder (Isay 1970). To solve the coupled system, the problem is solved iteratively in the method developed by Krüger (2018). Starting at the propeller, the circulation of the propeller, its self induced velocities and the induced velocities at the next device downstream are calculated. Then the circulation and self induced velocities of this device and the induced velocities of the device on the other lifting devices, up- and downstream, are calculated. This procedure is carried out until the results are converged. As all lifting devices, represented by their bound and free vortices, are calculated in one setup, the final solution includes the bi- or multidirectional (depending on the number of devices) interaction between the lifting lines.

2.2 Panel Method

The used panel method is based on the work of Söding (1997) and is being improved in an ongoing process since then. This panel method is a desingularised direct panel method, which means that the equations are set up to solve directly for the flow potential and that the singularities of the panels are located inside the body behind the panels. Within the method, the body is discretised by panels with point doublets and sources, whereas the wake behind the sharp trailing edge is discretised by wake panels without any thickness. The total number of panels is denoted in this paper as n_p, which is the sum of all body panels n_b and all wake panels n_w.

The geometry of the wake is initially unknown, whereas it is crucial for an accurate calculation. Katz & Plotkin (2001) and, later for a different setup, Bissonnette & Bramesfeld (2017) showed that especially the induced drag depends on the wake geometry, while it has only a minor influence on the lift. However, the calculation of the wake shape of a rudder in the propeller slipstream is very challenging as it has a complex strongly deformed geometry (as later shown in fig. 2). Moreover, the results depend strongly on the position and shape of the wake. This dependence between the results and the shape of the wake makes iterative approaches converge slowly or sometimes even lets them diverge, which leads to the requirement of an accurate initial calculation of the wake shape. As an approximation, the wake is often modelled as a plane with half of the angle of attack of the lifting device, which leads to satisfying results in the lift, but has drawbacks in the drag and centre of pressure prediction.

The equation system of the panel method is derived from Green's second identity (Söding 1997):

$$\int_{S_b+S_w} \phi\left(\vec{x}\right) \frac{\partial}{\partial n} G\left(\vec{x},\vec{x}_0\right) \mathrm{d}S = \int_{S_b} \vec{U}\cdot\vec{n} G\left(\vec{x},\vec{x}_0\right) \mathrm{d}S \tag{8}$$

With the Green function G, which corresponds to a source of strength 4π:

$$G\left(\vec{x},\vec{x}_0\right) = \frac{1}{|\vec{x}-\vec{x}_0|} \tag{9}$$

In equation (8) S_b denotes the surface of the body and S_w the surface of the wake. $\phi\left(\vec{x}\right)$ is the potential at the point $\vec{x}$. The inflow velocity at a panel is denoted by $\vec{U}$ and the normal vector of the panel by $\vec{n}$. The vector $\vec{x}_0$ describes the location of the collocation points. The equation leads to a dense $n_b \times n_b$ matrix, with the potential of the body panels as the unknown vector.

When calculating a rudder in the propeller slipstream, the inflow vector field $\vec{U}$ is not free of rotation. As stated by Söding (1997), the application of the inflow in this way as a Kutta condition is a violation of the principle of vanishing rotation inside a potential fluid. But despite this, as also stated, the method delivers satisfying results.

After solving the linear equation system, the potential of the rudder can be calculated at any position in the fluid $\vec{x}_0$:

$$\phi\left(\vec{x}_0\right) = \sum_{i=1}^{n_p} \Bigg(\phi_i \int \nabla G(\vec{x},\vec{x}_0)\vec{n}\mathrm{d}S - \nabla\phi_i\vec{n}\int G(\vec{x},\vec{x}_0)\mathrm{d}S \Bigg) /4\pi \tag{10}$$

where ϕ_i is the solution of the equation system (8) for the panel i.

Thereafter, the velocity $\vec{U}$ is calculated with the gradient of the potential, which is numerically calculated with central differences:

$$\begin{aligned}\vec{U} &= \begin{pmatrix} u \\ v \\ w \end{pmatrix} = \nabla\phi\left(\vec{x}_0\right) \\ &= \frac{1}{2\epsilon}\begin{pmatrix} \phi\left(x+\epsilon,y,z\right) - \phi\left(x-\epsilon,y,z\right) \\ \phi\left(x,y+\epsilon,z\right) - \phi\left(x,y-\epsilon,z\right) \\ \phi\left(x,y,z+\epsilon\right) - \phi\left(x,y,z-\epsilon\right) \end{pmatrix} + O(\epsilon^2)\end{aligned} \tag{11}$$

Where ϵ is a small distance and O is the error of the numerical implementation, which is a function of the squared distance.

The circulation Γ, which is of special importance later in the procedure, is defined as the velocity along a closed curve (Schlichting & Truckenbrodt 1967):

$$\Gamma = \oint \left(u\mathrm{d}x + v\mathrm{d}y + w\mathrm{d}z\right) \tag{12}$$

Schlichting & Truckenbrodt (1967) show that the circulation of a section is the difference of the potential at the trailing edge between the suction side $\phi_{GP,te,1}$ and the pressure side $\phi_{GP,te,2}$:

$$\Gamma(z) = \phi_{GP,te,1}(z) - \phi_{GP,te,2}(z) \tag{13}$$

As the potential is generally calculated for the centre of each panel, the potential at the grid points ϕ_{GP} is calculated as the average of the surrounding panels. The potential at the grid points on the trailing edge of the rudder $\phi_{GP,te}$ needs to be calculated more accurately, which is why the potential there is not calculated using the average, but by linear extrapolating from the potential of the grid points on the surface.

3 COUPLED CALCULATION

The procedure of the coupled method is shown in figure 1. During the initialisation the user defines his calculation setup. Moreover, all necessary data from the ship is obtained, as e.g. the propeller geometry, rudder geometry and resistance curve.

Thereafter, the calculation starts with the lifting line procedure. Here, the propeller circulation is determined starting with no induced velocities. During the calculation of the circulation of the propeller, the velocities at the position of the bound vortex (see equations (2) and (3)) are calculated. Afterwards, the induced velocities at the rudder are determined. Now, the circulation of the rudder, also represented by a lifting line, is calculated using the induced velocities of the propeller but starting with no self induced velocities. After calculating the rudder circulation, the self induced velocities are known and the rudder induced velocities at the propeller can be calculated. The first iteration in the lifting line procedure ends here and starts with a new iteration step. The lifting line procedure converges quickly and delivers satisfying results after few iterations.

After the part of the lifting line converged, the velocities of the propeller and thus the pitch of the free vortices (see eq. (6)) at the trailing edge of the rudder are used as an input for the panel method. The mentioned velocities include the surrounding flow velocity and the propeller induced velocities for points inside the propeller slipstream. These velocities are used to set up the equation system of the panel method (EQS). Here, as already stated in section 2.2, an error is made as the inflow field from the propeller to the rudder is not free of rotation, which is a violation of the assumptions of a potential flow. Nevertheless, the impact of this error is estimated small and the method delivers results with satisfying accuracy (Söding 1997). The inflow on the body panels is needed for the requirement of vanishing flow through a panel (right hand side of equation (8)). The pitch of the free vortex system calculated in the lifting line procedure is used for the wake panels of the rudder, which are aligned parallel to the flow coming from the lifting line.

Independent from the input of the lifting line, the geometry of the rudder and, if present, of the skeg is generated. In the used method a structured grid is used for computation. With the aforementioned steps in the panel method, all data is known to set up the equation system of the panel method, which is subsequently solved for the source strength ϕ (see eq. (8)).

The last step in the panel method is the evaluation. Here, the velocities on the body panels are calculated and thereafter the pressure on each panel is calculated by Bernoulli's principle. By multiplying with the area of a panel and afterwards summing up the forces of all panels, the rudder forces are obtained.

Now, the results of the panel method are used to improve the results of the lifting line. The circulation of the rudder is calculated as stated in equation (13). The induced velocity in x-direction in the propeller plane is calculated by equation (10) and (11). The velocities are calculated for several points inside the propeller plane and consequently the circumferential average is taken for each radius. With this improved results from the panel method, a new iteration step is started from the lifting line.

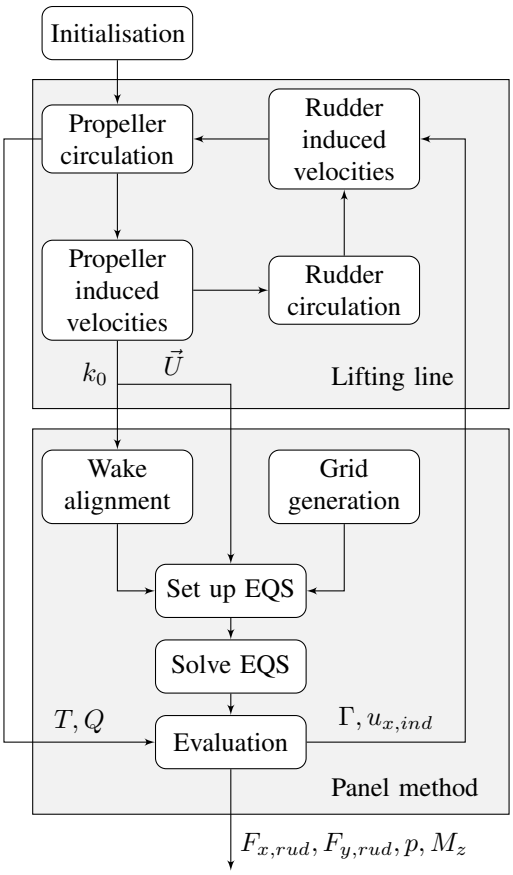

Figure 1: Simplified flowchart of the coupled method.

4 RESULTS

To show the effects of the coupling, a ship with small distance between rudder and propeller was chosen. The vessel is a twin screw vessel which runs $v = 21\,\text{kn}$ and has a four bladed propeller with a diameter of $D = 5\,\text{m}$. The distance from propeller plane to the leading edge of the rudder is $x/D = 0.3$. The rudder is, for this investigation, a symmetric spade rudder with a costa bulb. All calculations presented in this chapter are carried out for an advance coefficient of $J = 0.9$ and a rudder angle of $\delta = 0°$. The rudder angle of $\delta = 0°$ is of special interest for the energy efficiency and to find the operating point.

The results of the lifting line part are visualised by the propeller and rudder and their corresponding free vortex system in figure 2. The profiles of the rudder and propeller are just shown for a better understanding, as the lifting bodies are just lines in the scope of the method. The deformation of the free vortex sheet of the rudder due to the inflow from the propeller can be seen on the right hand side. Furthermore, the lower pitch of the free vortices at the tip of the propeller are clearly seen after one and a half rotations.

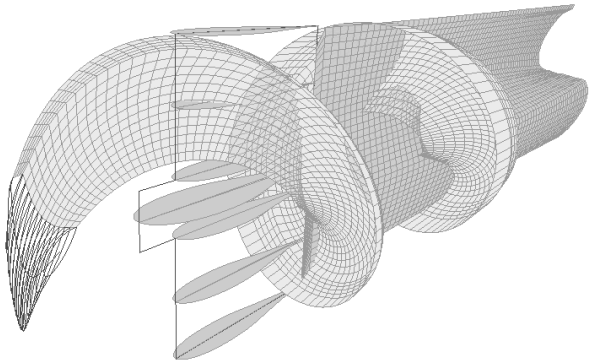

Figure 2: Visualisation of the helical wake behind the propeller and the deformed axial wake behind the rudder calculated with the lifting line approach.

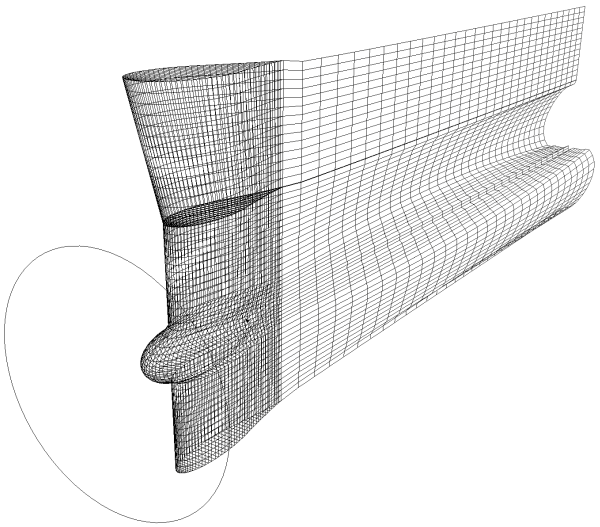

Figure 3: Visualisation of the grid used in the panel method.

The results of the lifting line are used for the wake geometry in the panel method, which is depicted in figure 3. The rudder is discretised by 40 panels in axial direction on both sides of the rudder and by 40 panels in vertical direction. The skeg above the rudder has the same spacing in axial direction and 14 panels in vertical direction. The top and bottom of the rudder and skeg is closed with one panel in transversal and a to the sides corresponding number of panels in axial direction. The wake geometry consists of 30 wake panels in the flow direction. In vertical direction the discretisation is the same as on the body, as each body panel has one corresponding wake sheet.

Before evaluating the forces, a closer look should be given at the induced velocities by the rudder at the position of the propeller plane, depicted in figure 4. The induced velocities calculated in the lifting line method have solid lines, while the induced velocities calculated using the panel method are dashed. The figure shows the benefit of the presented coupling. The axial velocity calculated in the lifting line $v_{x,LL}$ is close to zero, as the lifting line has no thickness and just a induces a small velocity due to the circulation of the rudder. The panel method on the other hand, capable to calculate the effect of the thickness, can calculate the induced axial velocity $v_{x,PM}$ at the propeller. On the contrary, the tangential velocity calculated using the panel method $v_{t,PM}$ is zero at all radii. As the flow in the panel method is assumed to be free of rotation, the circumferential average of the tangential velocity needs to be zero according to the Stokes' theorem, if the closed integral does not include a singularity. In consequence of the violation of vanishing rotation when applying the inflow from the propeller in the panel method (see section 2.2), the flow field is not free of rotation although there are no singularities inducing the rotation. However, due to the lack of singularities the flow field is assumed to be free of rotation in the panel method. As a result of this error, no averaged circumferential velocity is induced by the rudder at the propeller plane.

In contrast, the multi-component lifting line method is capable to calculate the tangential velocity $v_{t,PM}$, as it integrates the equation of Biot-Savart (see eq. (1)) directly for points upstream of the lifting device. As the lifting line method considers the interaction between both lifting devices, the free vortices of the propeller are part of the solution of the rudder. Therefore, singularities are present at the propeller plane when calculating the averaged induced circumferential velocity of the rudder at the propeller plane. Consequently, the averaged circumferential induced velocity of the rudder at the propeller plane does not vanish in the lifting line calculation, see (Brunnstein 1968), (Isay 1970) and (Krüger 2018).

The radial velocity v_r is only depicted for the panel method ($v_{r,PM}$) and not for the lifting line, because it is not used within the lifting line procedure as a result of simplifications (Isay 1964). Furthermore, a calculation of the radial velocity in the lifting line method would strongly underestimate the magnitude of the velocity as the finite thickness of the rudder is not taken into account in the lifting line.

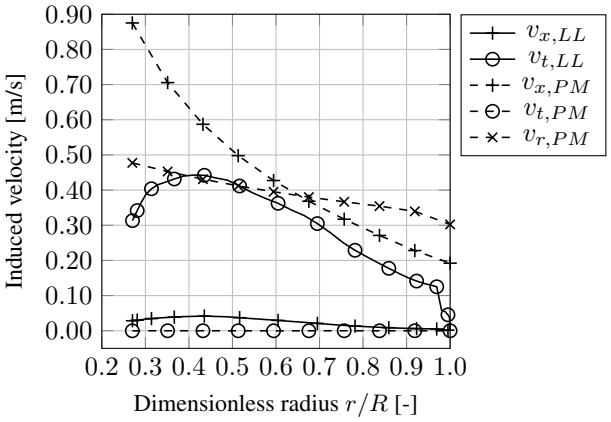

Figure 4: Induced velocities by the rudder at the propeller plane.

Figure 5 shows the circulation of the rudder. On the abscissa, the z-coordinate of the rudder is mapped to a dimensionless radius $r/R = (z - z_{shaft})/R$, with R being half the propeller diameter. The initially calculated circulation in the lifting line Γ_{LL} is nearly symmetric. The circulation calculated using the panel method in the first step of the iteration $\Gamma_{PM,1}$ is on the lower half of the rudder just slightly bigger than the circulation calculated previously with the lifting line. The circulation is especially a little bit shifted to the lower end. On the upper half of the rudder, the skeg prevents a flow around the upper edge of the rudder which leads to higher circulations on the upper half of the rudder. As the lifting line is not capable to consider the skeg, the circulation is much larger in the panel method as in the lifting line. Afterwards, the circulation between the first $\Gamma_{PM,1}$ and third iteration step $\Gamma_{PM,3}$ only change little.

The forces calculated with the different methods and for steps in between are shown in table 1. In the first row, the results of the panel method with a one way coupling are presented. The thrust and torque are calculated with a lifting line approach for a free running propeller and the velocities in the slipstream of this propeller are handed to the panel method as the inflow.

The second row presents the results of the lifting line procedure (upper rectangle in fig. 1). Both, the propeller and the rudder, are represented by a lifting line and interact with each other. The transversal rudder force is very small, as the skeg is not taken into account in this procedure. The longitudinal rudder force is calculated based on tabulated values from the profile theory. The thrust and torque of the propeller increase compared to the free running propeller mainly because of the induced transversal velocity at the propeller (see fig. 4).

As stated in the previous section, the results of the lifting line are handed to the panel method. The results when reaching the *Evaluation* block (see fig. 1) for the first time are shown in the line *Coupled, step 1*. As the propeller forces were not recalculated, they are the same as in the coupled lifting line. The magnitude of the longitudinal and transversal rudder forces increase compared to the first line. Hereby, the relative change in the axial forces is larger than the relative change in the transversal forces.

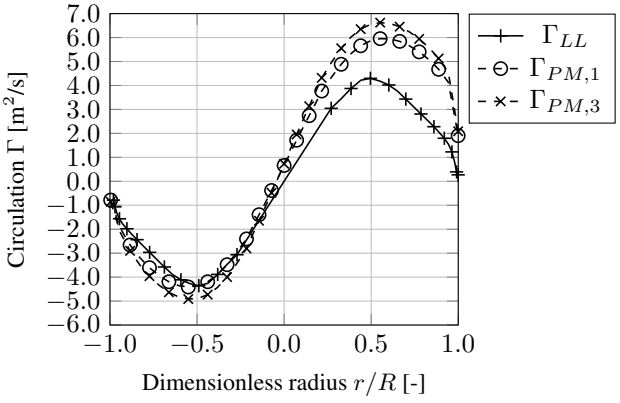

Figure 5: Circulation of the rudder.

Table 1: Calculated forces for the port side rudder.

Method	$F_{y,rud}$ [kN]	$F_{x,rud}$ [kN]	T [kN]	Q [kNm]
Panel method	-47.3	2.5	472.9	464.5
Lifting line	1.0	-13.6	504.5	492.2
Coupled, step 1	-49.3	4.5	504.5	492.2
Coupled, step 2	-53.5	7.5	550.7	529.1
Coupled, step 3	-53.9	7.8	554.2	532.2

The results after returning the values from the panel method back to the lifting line and again reaching the *Evaluation* block are found in the line *Coupled, step 2*. The magnitude of the longitudinal and transversal rudder forces increase compared to the previous iteration step. Moreover, the propeller thrust and torque increase, but here mainly due to the induced axial velocity which lets the propeller work at a lower advance coefficient. The amount of the increase is in good accordance with the measurements presented by Molland & Turnock (1993), where a similar setup with a distance of $x/D = 0.34$ was analysed. For a comparable advance coefficient, an increase in thrust and torque of approximately 13% in thrust and 16% in torque was found. In the presented calculation, the increase from the free running propeller to the coupled system amounts to 16% in thrust and 14% in torque.

In the last iteration step the forces only change little and the procedure can be considered as converged.

CONCLUSIONS

By coupling a lifting line method with a panel method, a fast procedure for the calculation of rudder-propeller-interaction was presented. The method runs quick enough to be executed on the personal computer and to be used within the design process.

The comparison to results of a similar case from the literature showed good accordance, while a validation is still pending and scheduled later this year. Further improvements are planed on the side of the lifting line to calculate the axial induced velocity based on the profile theory. This improvement would lead to a better initial calculation of the lifting line and would speed up the subsequent iteration in the coupled method.

ACKNOWLEDGEMENT

The method presented has been developed as part of the research project ESD@SEA, which aims at the design of energy saving devices for real operating conditions. Many thanks are due to the German Federal Ministry of Economic Affairs and Energy (BMWi) for funding this project. I would also like to thank Prof. Krüger for his support and supervision.

REFERENCES

Berger, S., Scharf, M., Göttsche, U., Neitzel, J. C., Angerbauer, R. & Abdel-Maksoud, M. (2015). 'Numerical simulation of propeller-rudder interaction for non-cavitating and cavitating flows using different ap-

proaches'. Fourth International Symposium on Marine Propulsors smp'15, Austin, Texas.

Bissonnette, W. & Bramesfeld, G. (2017). 'Effects of wake shapes on high-lift system aerodynamic predictions'. Aerospace **4**(2).

Brunnstein, K. (1968). Wechselwirkung zwischen Schiffsnachstrom, Schraubenpropeller und Schiffsruder [Interaction between ship wake, screw propeller and ship rudder]. Dissertation, Universität Hamburg, Ber. Nr. 210 Institut für Schiffbau der Universität Hamburg, Hamburg.

Goldstein, S. (1929). 'On the vortex theory of screw propellers'. Proceedings of the Royal Society of London, **123**, pp. 440–465.

Isay, W. H. (1964). Propellertheorie : hydrodynamische Probleme [Propeller theory: hydrodynamic problems]. Berlin: Springer.

Isay, W. H. (1970). Moderne Probleme der Propellertheorie [Modern problems of propeller theory]. Berlin: Springer.

Katz, J. & Plotkin, A. (2001). Low-speed aerodynamics. 2nd ed. Cambridge: Cambridge Univ. Press.

Krüger, S. & Abels, W. (2017). 'Hydrodynamic damping and added mass of modern screw propellers'. OMAE, Trondheim, Norway.

Krüger, S. (2018). 'Computation of the free vortex system of multi component propulsors'. Ship Technology Research **66**(1), pp. 1–8.

Lerbs, H. (1955). Über gegenläufige Schrauben geringsten Energieverlustes im Nachstrom [On contra rotating screws of lowest energy loss in wake]. Schiffstechnik **9**, pp. 113–122.

Li, D.-Q. (1996). 'A non-linear method for the propeller-rudder interaction with the slipstream deformation taken into account'. Computer Methods in Applied Mechanics and Engineering **130**(1), pp. 115 – 132.

Molland, A. & Turnock, S. (1993). 'Wind tunnel investigation of the influence of propeller loading on a semi-balanced skeg rudder'. Ship Science Reports **48**.

Molland, A. F. & Turnock, S. R. (2007). Marine rudders and control surfaces : principles, data, design and applications. Amsterdam: Butterworth-Heinemann.

Prandtl, L. & Betz, A. (1927). 'Vier Abhandlungen zur Hydrodynamik und Aerodynamik' [Four treatise on hydrodynamics and aerodynamics]. ZAMM - Zeitschrift für Angewandte Mathematik und Mechanik **8**(1), pp. 9–67.

Schlichting, H. & Truckenbrodt, E. (1967). Aerodynamik des Flugzeuges [Aerodynamic of the aeroplane], vol. 1, 2nd ed. Berlin: Springer.

Söding, H. (1993). 'Rudders, fundamental hydrodynamic aspects'. In Brix, J. E.(ed.), Manoeuvring technical manual, Hamburg: Seehafen-Verlag.

Söding, H. (1997). 'Limits of potential theory in rudder flow prediction'. Ship Technology Research **45**(3).